Extracting connectivity from dynamics of networks with uniform bidirectional coupling

Emily S. C. Ching,[1,*] Pik-Yin Lai,[2,†] and C. Y. Leung[1]

[1]*Department of Physics, The Chinese University of Hong Kong, Shatin, Hong Kong*

[2]*Department of Physics, Graduate Institute of Biophysics, and Center for Complex Systems, National Central University, Chungli, Taiwan 320, Republic of China*

(Received 17 June 2013; revised manuscript received 12 September 2013; published 25 October 2013)

In the study of networked systems, a method that can extract information about how the individual nodes are connected with one another would be valuable. In this paper, we present a method that can yield such information of network connectivity using measurements of the dynamics of the nodes as the only input data. Our method is built upon a noise-induced relation between the Laplacian matrix of the network and the dynamical covariance matrix of the nodes, and applies to networked dynamical systems in which the coupling between nodes is uniform and bidirectional. Using examples of different networks and dynamics, we demonstrate that the method can give accurate connectivity information for a wide range of noise amplitude and coupling strength. Moreover, we can calculate a parameter Δ using again only the input of time-series data, and assess the accuracy of the extracted connectivity information based on the value of Δ.

DOI: 10.1103/PhysRevE.88.042817 PACS number(s): 89.75.Hc, 05.45.Tp, 05.45.Xt

I. INTRODUCTION

The study of networked systems, namely, systems that consist of a number of elementary components, known as nodes, interacting with one another, has become increasingly important in many disciplines including physics, biology, and social science (see, for example, reviews [1–3]). The collective behavior of these systems would arise from the interactions of the nodes. Thus to understand these systems or networks, it is important to know how the individual nodes interact. When the dynamics of a node depend explicitly on that of another node, the latter node is connected or linked to the former node. For many biological networks, knowing the network connectivity, i.e., how the nodes are connected and interacting with one another, is a significant first step for understanding the functionality of the networks. Hence extracting network connectivity from measurements of the dynamics of the nodes has become an active area of research and has direct relevance in many fields.

The problem is generally difficult and efforts have been mostly focused on networks that are modeled by dynamical systems with the time evolution described by a set of differential equations. A method exploiting stationary response properties of networks to applied external driving has been proposed [4]. It was shown that this method could yield network connectivity by measuring the responses to sufficiently many suitable driving conditions in networks of coupled phase oscillators. In another method [5], a second network with the same intrinsic dynamics of the individual nodes and the same interaction dynamics among the nodes as the original network of interest is introduced. The network connectivity of the second network is varied such that its dynamics synchronizes with the original one then the connectivity of the second network is recognized as that of the original network. This method thus requires the functional forms of both the intrinsic dynamics and interaction dynamics to be known. It has later been shown that [6] when these functional forms are known, network connectivity can be obtained directly from the measured time-series data of the nodes. In a related study [7], a coupled leaky integrate-and-fire model of neurons is used. The parameters of the model, including those describing the connectivity, are determined by minimizing the difference between the spiking data generated from this model and the measured spike train data of a neuronal network. The resulting model with its connectivity information is taken to represent the original neuronal network of interest. A recent work [8] shows that the presence of noise in certain networked systems leads to a relation between the dynamical covariance of the measurements of the nodes and the connectivity of the nodes. This noise-bridging relation has been exploited [8,9] for network reconstruction with an explicit use of the amplitude of the noise and the strength of the coupling between nodes. Thus all these earlier studies require information in addition to the dynamics of the nodes for the extraction of the connectivity of the network.

In this paper, we shall present a method that extracts network connectivity using solely measurements of the dynamics of the nodes. Our present study focuses on networked dynamical systems in which coupling between nodes is bidirectional and with uniform coupling strength. Our method is built upon the mathematical relation between the dynamical covariance and the connectivity discussed above. The paper is organized as follows. In Sec. II, we shall set up the problem and review the work presented in [8]. In particular, an exact mathematical relation between dynamical covariance and connectivity can be derived for networks with linear diffusive coupling between nodes and individual nodes having no intrinsic dynamics. The direct derivation is given in the Appendix. Then, in Sec. III, we shall discuss how we can eliminate any explicit reference to the noise amplitude σ and coupling strength g in the mathematical relation to devise a method that extracts network connectivity using measurements of the dynamics as the only input data. Moreover, we can calculate a parameter Δ using again only the measured dynamical data, and assess

*ching@phy.cuhk.edu.hk

†pylai@phy.ncu.edu.tw

the accuracy of the extracted connectivity information based on the value of Δ. We have applied our method to different types of networks with linear diffusive coupling between nodes including systems whose nodes have intrinsic dynamics. The performance of such a method can be evaluated by comparing the extracted connectivity against the actual one. In Sec. IV, we compare the extracted and the actual connectivity using different measures, and assess quantitatively the performance of our method. Our results demonstrate that the method can give accurate connectivity information for a wide range of values of σ and g even for systems with intrinsic nonlinear dynamics. We also explore the possibility of estimating σ^2/g again using only the measured dynamical data. Finally, we end the paper with a conclusion and outlook for future work.

II. PROBLEM

We consider a networked dynamical system of N nodes, whose time evolution is described by the following set of coupled differential equations:

$$\dot{x_i} = f(x_i) + \sum_{j=1}^{N} g_{ij} A_{ij} h(x_i, x_j) + \eta_i \tag{1}$$

for $i = 1,2,3\ldots,N$. Here, x_i denotes the state variable of the ith node, and the time series $x_i(t)$ can be measured. The function f describes the intrinsic dynamics of the individual nodes and is taken to be identical for all the nodes. When $\dot{x_i}$ is a function of $x_j(t)$ with $j \neq i$, the jth node is said to be connected or linked to the i node, then $A_{ij} = 1$ and the interaction between the two nodes i and j is described by the coupling function $h(x_i, x_j)$. Otherwise, $A_{ij} = 0$. Together with the definition $A_{ii} \equiv 0$, A_{ij} gives the component of the adjacency matrix $\hat{A}$. g_{ij} is the coupling strength of the link from the jth node to ith node. η_i is a Gaussian white noise with zero mean and variance σ^2:

$$\overline{\eta_i(t)\eta_j(t')} = \sigma^2 \delta_{ij}\, \delta(t - t'), \tag{2}$$

where the overbar is an average over noise. In this paper, we confine our study to networked dynamical systems with uniform bidirectional coupling such that $\hat{A}$ is symmetric and $g_{ij} = g$. Moreover, we consider networks whose graphs have only one connected component. The problem that we would like to address is the following. How can $\hat{A}$, which specifies the connectivity of the network, be extracted solely from the measurements $x_i(t)$ of the dynamics of the system?

For the case of linear diffusive coupling, $h(x_i, x_j) = x_j - x_i$, and negligible intrinsic dynamics, $f(x_i) \approx 0$, Eq. (1) becomes

$$\dot{x_i} = g \sum_{j=1}^{N} A_{ij}(x_j - x_i) + \eta_i = -g \sum_{j=1}^{N} L_{ij} x_j + \eta_i. \tag{3}$$

Dynamics described by Eq. (3) is known as the consensus dynamics [10], and L_{ij} are the components of the Laplacian matrix $\hat{L}$, defined by

$$L_{ij} \equiv k_i \delta_{ij} - A_{ij} \tag{4}$$

and

$$k_i \equiv \sum_{j=1}^{N} A_{ij} \tag{5}$$

is the in degree of the ith node measuring the number of connections or links to the ith node, which is also the out degree of the ith node for bidirectional networks. Thus we refer k_i simply as the degree of the ith node. Note that

$$\sum_{j=1}^{N} L_{ij} = \sum_{i=1}^{N} L_{ij} = 0. \tag{6}$$

Thus $\hat{L}$ has a null eigenvalue and is not invertible. Define the components C_{ij} of the dynamical covariance matrix $\hat{C}$ by

$$C_{ij} = \langle \overline{[x_i(t) - X(t)][x_j(t) - X(t)]} \rangle, \tag{7}$$

where $X(t) \equiv (1/N)\sum_{i=1}^{N} x_i(t)$, $\langle \cdots \rangle$ is an average over a time period T with $T \to \infty$, and $\overline{\cdots}$ denotes an average over the noise. A relation between $\hat{L}$ and $\hat{C}$,

$$\hat{C} = \frac{\sigma^2}{2g} \hat{L}^{+}, \tag{8}$$

was presented in Ref. [8]. Here, the superscript $+$ denotes the pseudoinverse of a matrix. This result is exact for the specific case of a networked system with consensus dynamics described by Eq. (3). We shall give a direct derivation in the Appendix.

Equation (8) implies

$$\hat{L} = \frac{\sigma^2}{2g} \hat{C}^{+}, \tag{9}$$

which shows that the network connectivity, as specified by $A_{ij} = -L_{ij}$ for $i \neq j$, is given by $-\sigma^2/(2g)C_{ij}^{+}$. This result is exact in the limit of averaging over infinite time. In any practical calculation of C_{ij}, the time averaging is, however, carried out over a finite period of time and only for data obtained in one particular realization of the noise. As a result, the calculated values of $\sigma^2/(2g)C_{ij}^{+}$ instead display a bimodal distribution with two peaks around 0 and -1 and an overlap between the two peaks is possible. An approximate result for the degree of a node has been used [8] to separate the calculated values of $\sigma^2/(2g)C_{ij}^{+}$ for $i \neq j$ into two groups, one associated with $A_{ij} = 1$ and the other with $A_{ij} = 0$. As σ and g appear explicitly in the calculations of both $\sigma^2/(2g)C_{ij}^{+}$ and the approximate result for the degree of a node, this method thus requires the knowledge of the noise strength as well as the coupling strength. However, such knowledge is likely to be lacking in practical problems. Thus a desirable method would be one that extracts network connectivity using only the measurable time-series data $x_i(t)$, $i = 1,2,\ldots,N$ of the nodes. To devise such a method, one needs to eliminate any reference to the *a priori* unknown quantities σ and g. We shall discuss how this can be achieved in the next section.

III. METHOD

From Eqs. (4) and (9), we have

$$\frac{\sigma^2}{2g}C_{ii}^{+} = k_i, \tag{10}$$

$$\frac{\sigma^2}{2g}C_{ij}^{+} = -A_{ij}, \quad i \neq j. \tag{11}$$

As the factor $\sigma^2/(2g)$ appears in both Eqs. (10) and (11), it can be eliminated by taking the ratio of the diagonal and off-diagonal elements of $\hat{C}^{+}$. Defining

$$r_{ij} \equiv \frac{C_{ij}^{+}}{C_{ii}^{+}}, \quad i \neq j, \tag{12}$$

then

$$r_{ij} = \begin{cases} 0, & \text{nodes } i \text{ and } j \text{ are not connected,} \\ -\frac{1}{k_i}, & \text{nodes } i \text{ and } j \text{ are connected.} \end{cases} \tag{13}$$

Thus the information about the connectivity is contained completely in the r_{ij}'s, which can be calculated using only the dynamical time series $x_i(t)$ of the nodes. For a given node i, the values of r_{ij}'s would separate into two groups: group 1 of values close to 0 and group 2 of negative values close to $-1/k_i$. With this separation, the nodes j with r_{ij}'s in group 2 can be deduced to be connected to node i, while those in group 1 are not connected to node i. As discussed earlier, in realistic situations, the calculation of the elements C_{ij} would be done with an averaging in time over a finite interval and without any average over the noise. Because of this, Eq. (9) and thus Eq. (13) would not hold exactly. As a result, the separation of the r_{ij}'s into two groups could be much less distinct. We outline a procedure below that allows us to make such a separation in realistic situations.

(1) Calculate r_{ij} for $i = 1, \ldots, N$ and $j \neq i$.

(2) For a given node i, arrange the $N-1$ values of r_{ij} in ascending order and denote them as $r_i(m)$, with $r_i(1)$ being the smallest value of r_{ij}. From Eq. (13), we expect that for nodes that are connected to i, $r_i(m) < 0$ and are close to one another. Then when we get to nodes that are unconnected to node i, we expect to see a big difference in $r_i(m)$ of the order $1/k_i$. Thus a relatively big difference between $r_i(m+1)$ and $r_i(m)$ should occur at a certain value $m = m_0(i)$. By identifying $m_0(i)$, we can deduce that nodes j with r_{ij} corresponding to $r_i(m)$ for $1 \leqslant m \leqslant m_0(i)$ $[m_0(i)+1 \leqslant m \leqslant N-1]$ are connected (unconnected) to node i. We identify $m_0(i)$ as the value m at which the largest value of $d_i(m) \equiv r_i(m+1) - r_i(m)$ occurs provided the following two conditions are satisfied: (i) the largest value of $d_i(m)$ is larger than two times the second-largest value and (ii) $r_i[m_0(i)] < 0$. These conditions are set to avoid getting spurious result.

(3) In the event that the above two conditions are not all satisfied, we take $m_0(i)$ to be the value m such that $\sum_{n=1}^{m} r_i(n)$ is closest to -1. This is based on the result that Eq. (13) implies that the sum of r_{ij} over those nodes j that are connected to node i is -1.

(4) We can measure how well the values of r_{ij} are separated into two groups by comparing $d_i[m_0(i)]$ with the average separation, which is given by $[r_i(N-1) - r_i(1)]/(N-2)$. Thus we define

$$\delta(i) \equiv \frac{r_i[m_0(i)+1] - r_i[m_0(i)]}{[r_i(N-1) - r_i(1)]/(N-2)}. \tag{14}$$

The accuracy of the extracted connectivity information for node i is expected to be high when $\delta(i)$ is large enough.

(5) For any pair of nodes i and j, it is possible that their mutual connectivity information deduced using r_{im}, $m \neq i$, is different from that deduced using r_{jm}, $m \neq j$. In such an event, we compare $\delta(i)$ and $\delta(j)$ and follow the deduction information obtained from the node with the higher value of δ.

Using this method, we can then extract the connectivity of a network with uniform bidirectional coupling, based only on the input of the dynamical time series of its nodes. The actual connectivity is unknown in realistic problems, it is thus useful to have a measure of the expected accuracy of an extracted result of connectivity. As discussed, we expect the method to work well and give accurate extraction when $\delta(i)$ is large for all the nodes. Thus we measure the overall accuracy of the extracted connectivity for the whole network by

$$\Delta \equiv \frac{1}{N}\sum_{i=1}^{N}\delta(i). \tag{15}$$

IV. RESULTS AND DISCUSSION

We have first applied the method for systems described by Eq. (3) on three different networks: a random network of $N = 100$ with probability $p = 0.2$, the network of C. elegans neurons with $N = 279$ obtained from the Wormatlas database [11], and the BA scale-free network introduced by Barabási and Albert [12] with $N = 1000$ and a new node connecting to two existing nodes in each step. We take $g = \sigma = 1$. To investigate how the accuracy of the method might depend on the coupling and noise strength, we have studied additional different values of g and σ for the random network. We integrate Eq. (3) in time using the Euler method and obtain the time series $x_i(t)$ for $i = 1,2, \ldots, N$. In the calculation of C_{ij}, we average over a total time T_{av} with a sampling time interval of 5×10^{-4}. Unless otherwise stated, we use $T_{\text{av}} = 1000$ with a total of 2×10^6 data points for the average. To mimic real situations, no average over the noise is taken. Thus Eq. (13) only holds approximately as discussed in Sec. III. We have calculated the values of r_{ij} and arrange them in ascending order as $r_i(m), m = 1, \ldots, N-1$, for each node i as discussed. In Fig. 1, typical results for a certain node i for the random network with $g = \sigma = 1$ are shown. A clear separation of the values $r_i(m)$ into two groups can be seen. In this case, $\delta(i) = 21.0$.

Our method is based on the separation of the values of r_{ij}, $i \neq j$, into two groups according to whether nodes i and j are connected or not. Equation (9), which is derived for networked systems with consensus dynamics described by Eq. (3), provides the mathematical basis for such a separation. Although Eq. (9) has not been proved for systems with general dynamics, the work in Ref. [8] showed that there is an approximate separation of the values of $\sigma^2/(2g)C_{ij}^{+}$ into two groups even for systems with intrinsic Rössler dynamics [13]. This suggests that our method can be applicable even for

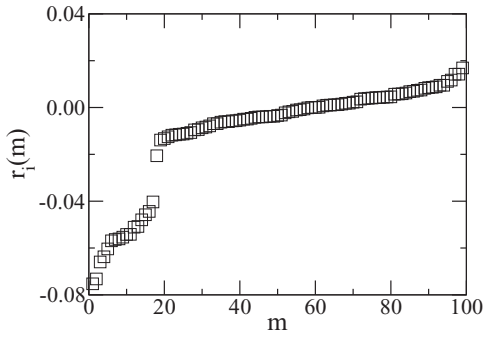

FIG. 1. Values of $r_i(m)$ as a function of m for a certain node i of the random network with $\sigma = 1$ and $g = 1$.

systems with nontrivial intrinsic dynamics. To investigate this, we have studied the same three networks with the FitzHugh-Nagumo (FHN) dynamics [14], which is commonly used to model oscillatory or excitable systems such as neurons or cardiac cells:

$$\dot{u_i} = \frac{1}{\epsilon}\left(u_i - \frac{u_i^3}{3} - v_i\right) + g\sum_{j=1}^{N} A_{ij}(u_j - u_i) + \eta_i, \quad (16)$$

$$\dot{v_i} = u_i + a, \quad (17)$$

with $\epsilon = 0.01$ and two values of a: 1.05 and 0.95. For the noise-free case with no coupling, i.e., $\eta_i = g = 0$, the nodes display excitable dynamics for $|a| > 1$ and oscillatory dynamics if $|a| < 1$. Coupled excitable FHN networks under noise display many interesting phenomena, such as coherence resonance [15,16] in which the nodes can exhibit rather regular periodic oscillations in some suitable noise regimes, and frequency enhancement [17] in which the interplay of coupling and noise give rise to nontrivial frequency variations. We denote excitable dynamics for $|a| > 1$ as FHN1 dynamics and oscillatory dynamics ($|a| < 1$) as FHN2 dynamics. We take $g = 10$ and $\sigma = 1$. For the random network, two additional sets of values, $g = 10$, and $\sigma = 0.1$ and $g = \sigma = 1$, have been studied. For the FHN1 and FHN2 dynamics, the equations of motion are similarly integrated, and we calculate the elements of the dynamic covariance matrix C_{ij} using $u_i(t)$'s, the time series for the fast variables, only.

Carrying out the procedure described in Sec. III, we have extracted the connectivity of the networks for all the cases studied. To assess the performance of the method, we compare the extracted values for the elements of the adjacency matrix, denoted as $A_{ij}^{(e)}$, with the actual values of A_{ij} using different measures. First, we focus on each node i and measure the accuracy of the method by $p_{\rm sen}(i)$ and $p_{\rm spec}(i)$, which are respectively the percentage of nodes that are correctly extracted to be connected to node i and the percentage of nodes that are correctly extracted to be unconnected to node i. That is, $p_{\rm sen}(i)$ and $p_{\rm spec}(i)$ measure the sensitivity and specificity of the method for node i in percentage. Denote the number of nodes that are correctly extracted to be connected to node i by $n_c(i)$ and the number of nodes that are correctly extracted to be unconnected to node i by $n_u(i)$. The number of connected nodes to node i is given by the degree of node i, k_i, while the number of nodes unconnected to node i is $N - 1 - k_i$. Thus

TABLE I. Overall sensitivity and specificity of the method for the different networks and dynamics.

Network	N	Dynamics	σ	g	$P_{\rm SEN}$	$P_{\rm SPEC}$
Random	100	Consensus	1	1	99.80	99.95
Random	100	FHN1	1	10	100	100
Random	100	FHN2	1	10	99.80	99.37
C. elegans	279	Consensus	1	1	99.87	99.98
C. elegans	279	FHN1	1	10	96.28	99.70
C. elegans	279	FHN2	1	10	98.21	99.32
BA scale-free	1000	Consensus	1	1	100	99.9996
BA scale-free	1000	FHN1	1	10	97.49	99.998
BA scale-free	1000	FHN2	1	10	96.69	99.999

$p_{\rm sen}(i)$ and $p_{\rm spec}(i)$ are defined as

$$p_{\rm sen}(i) = \frac{n_c(i)}{k_i} \times 100 = \frac{\sum_{j\neq i} A_{ij}^{(e)} A_{ij}}{\sum_{j\neq i} A_{ij}} \times 100, \quad (18)$$

$$p_{\rm spec}(i) = \frac{n_u(i)}{N-1-k_i} \times 100 = \frac{\sum_{j\neq i}\left(1 - A_{ij}^{(e)}\right)(1 - A_{ij})}{\sum_{j\neq i}(1 - A_{ij})} \times 100. \quad (19)$$

As A_{ij} is either 0 or 1, $A_{ij}^2 = A_{ij}$ and thus when $A_{ij}^{(e)} = A_{ij}$, we have $p_{\rm sen}(i) = p_{\rm spec}(i) = 100$ as it should be. The overall sensitivity and specificity of the method for the whole network are

$$P_{\rm SEN} = \frac{\sum_i n_c(i)}{\sum_i k_i} \times 100 = \sum_i p_c(i) p_{\rm sen}(i), \quad (20)$$

$$P_{\rm SPEC} = \frac{\sum_i n_u(i)}{\sum_i N-1-k_i} \times 100 = \sum_i p_u(i) p_{\rm spec}(i). \quad (21)$$

Thus the overall sensitivity and specificity, $P_{\rm SEN}$ and $P_{\rm SPEC}$, are the weighted averages of the sensitivity and specificity of the individual nodes, $p_{\rm sen}(i)$ and $p_{\rm spec}(i)$, with weights of $p_c(i)$ and $p_u(i)$, respectively:

$$p_c(i) \equiv \frac{k_i}{\sum_i k_i}, \quad (22)$$

$$p_u(i) \equiv \frac{N-1-k_i}{\sum_i N-1-k_i}. \quad (23)$$

Therefore, $P_{\rm SEN}$ is more affected by nodes with large degree, while $P_{\rm SPEC}$ is more affected by nodes with small degree. In Table I, we present the values of $P_{\rm SEN}$ and $P_{\rm SPEC}$ for the various cases studied. It can be seen that the accuracy of the method is generally very good with both $P_{\rm SEN}$ and $P_{\rm SPEC}$ being greater than 96. Moreover, $P_{\rm SPEC}$ is generally larger than $P_{\rm SEN}$ partly due to the average degree of the nodes being less than $N/2$ in all the three networks studied.

Next we look at $p_{\rm sen}(i)$ and $p_{\rm spec}(i)$ of the individual nodes in detail. In Fig. 2, we show the results for the three different types of dynamics for the random network. Similar results for the C. elegans and BA scale-free networks are shown in Figs. 3 and 4, respectively. The method is expected to work well particularly for networks with consensus dynamics. Almost perfect extraction is indeed obtained for all the three networks studied. For the random network, the method works

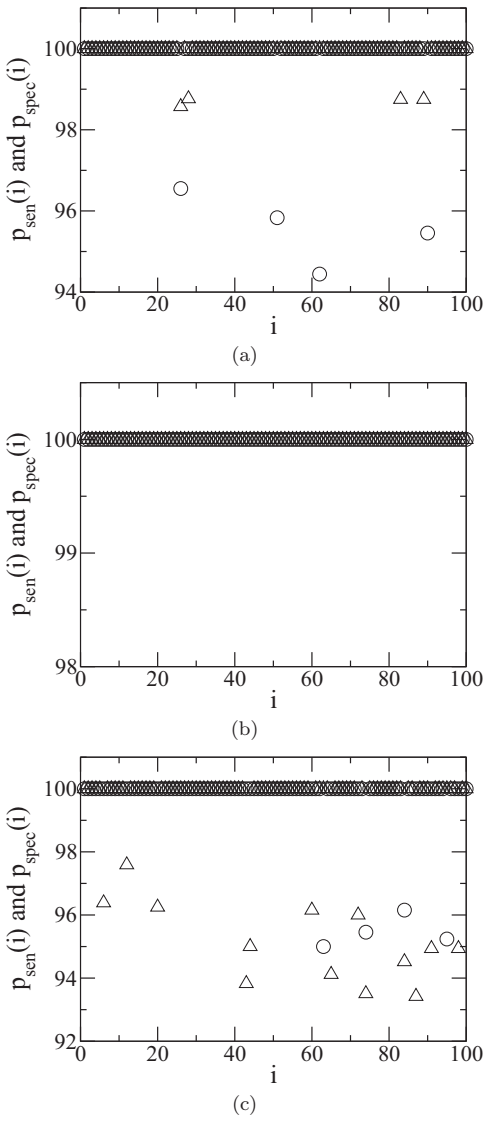

FIG. 2. $p_{\rm sen}(i)$ (circles) and $p_{\rm spec}(i)$ (triangles) for random network with (a) consensus dynamics with $\sigma = g = 1$, (b) FHN1 dynamics with $\sigma = 1$ and $g = 10$, and (c) FHN2 dynamics with $\sigma = 1$ and $g = 10$.

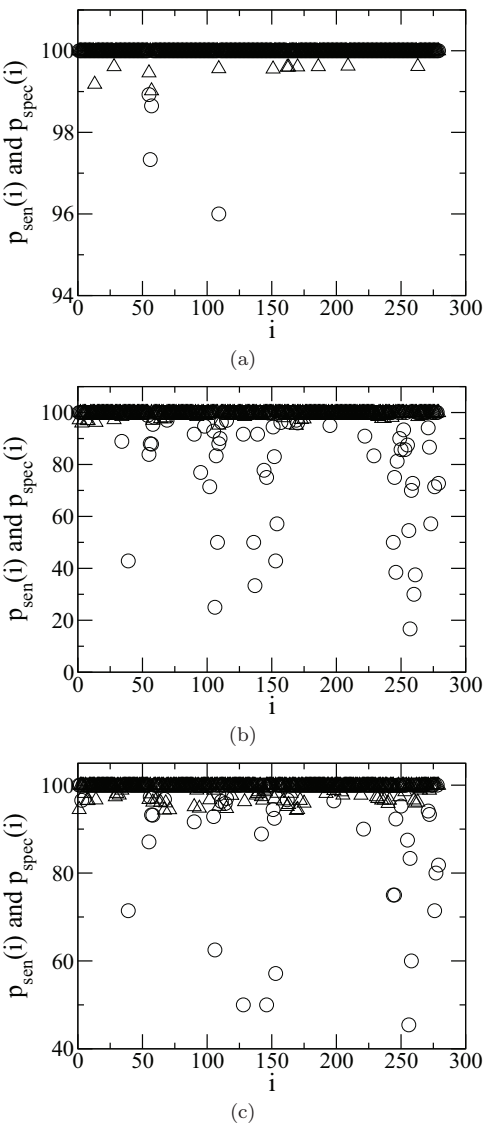

FIG. 3. Same as Fig. 2 for the C. elegans network.

very well too for the FHN1 and FHN2 dynamics. In particular, we have perfect extraction of $p_{\rm sen}(i) = p_{\rm spec}(i) = 100$ for the case of FHN1 dynamics. Thus the method can be applicable for general systems including systems whose nodes have nonlinear intrinsic dynamics. For the C. elegans and BA scale-free networks $p_{\rm sen}(i)$ is still larger than 70 for over 90% of the nodes for FHN1 and FHN2 dynamics.

We now discuss how $p_{\rm sen}(i)$ and $p_{\rm spec}(i)$ depend on the degree of the nodes. From Eq. (13), one expects $\delta(i) \sim 1/k_i$, and we have checked that this is the case on average using results for the BA scale-free network. A larger $\delta(i)$ would give rise to a smaller number of errors in the prediction. Thus we expect the number of errors to increase with the degree k_i on average. We can write $p_{\rm sen}(i)$ and $p_{\rm spec}(i)$ in terms of the number of errors. Specifically, $p_{\rm sen}(i) = [1 - (\text{number of errors})/k_i] \times 100$ and $p_{\rm spec}(i) = [1 - (\text{number of errors})/(N - k_i)] \times 100$. For the same number of errors, since $N - k_i > k_i$ in the networks that we have studied, $p_{\rm spec}(i)$ would be closer to 100 than $p_{\rm sen}(i)$. As can be seen in Figs. 2–4, this is indeed observed. Moreover, when $p_{\rm sen}(i)$ is plotted as a function of k_i, the data points would lie on curves of $[1 - (\text{number of errors})/k_i] \times 100$ with the number of errors increasing with k_i. As shown in Fig. 5, these features are confirmed.

Using the random network with consensus dynamics, we study how $P_{\rm SEN}$ and $P_{\rm SPEC}$ vary with g and σ. We find that the method works well for a wide range of σ and g. In particular, perfect extraction with $p_{\rm sen}(i) = p_{\rm spec}(i) = 100$ for all the nodes and thus $P_{\rm SEN} = P_{\rm SPEC} = 100$ is found for $g \geqslant 10$ and $0.1 \leqslant \sigma \leqslant 100$. We classify the result of extraction as satisfactory if both $P_{\rm SEN}$ and $P_{\rm SPEC}$ are greater than 95 and as unsatisfactory otherwise. In Fig. 6, we show the "phase diagram"of the performance of the method in the parameter space. It can be seen that the method works well when σ is larger than some threshold and when g is large. The threshold value of σ decreases as g increases. When g is small, one needs to average over very long time in order for Eq. (8) to hold. Therefore, for any value of σ and some fixed and finite $T_{\rm av}$, we

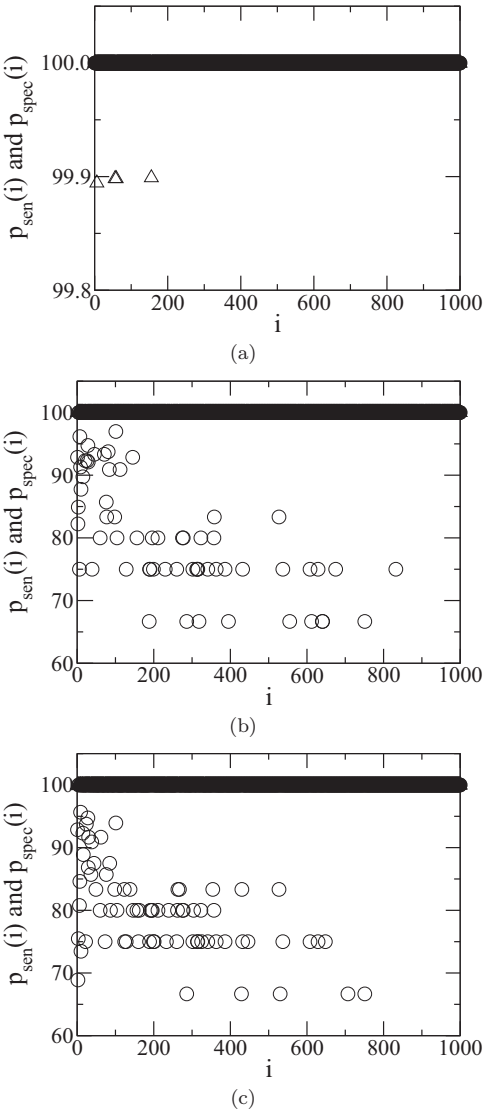

FIG. 4. Same as Fig. 2 for the BA scale-free network.

expect the values of $P_{\rm SEN}$ and $P_{\rm SPEC}$ to decrease as g decreases. Moreover, in the small-g regime, we expect the values of $P_{\rm SEN}$ and $P_{\rm SPEC}$ to increase when we increase $T_{\rm av}$. As can be seen in

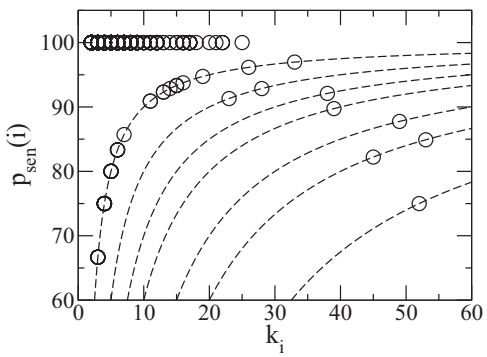

FIG. 5. Dependence of $p_{\rm sen}(i)$ on k_i for the BA scale-free network and FHN1 dynamics with $\sigma = 1$ and $g = 10$. The dashed lines are plots of $100[1 - (\text{number of errors})/k_i]$ with the number of errors being 1, 2, 3, 4, 6, 8, and 13 from left to right.

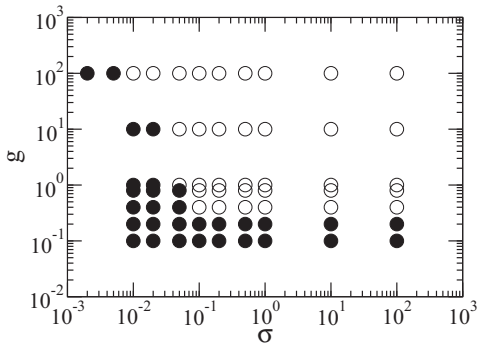

FIG. 6. Phase diagram showing the performance of the method in the parameter space for the random network with consensus dynamics with $T_{\rm av} = 1000$. Satisfactory results (both $P_{\rm SEN}$ and $P_{\rm SPEC}$ greater than 95) are represented by open circles, while unsatisfactory results are represented by closed circles.

Table II, all these expectations are confirmed. We have further checked that the value of $\delta(i)$, defined in Eq. (14), is indeed a good indicator of the accuracy of the extracted connectivity information of node i in general: $p_{\rm sen}(i)$ and $p_{\rm spec}(i)$ are close to 100 whenever $\delta(i)$ is sufficiently large. Hence the method is expected to give accurate extracted connectivity of the whole network when the value of Δ is sufficiently large. In the ideal situation when Eq. (13) holds, $\delta(i) = \Delta = N - 2$. We find that a good guideline of an accurate extraction is $\Delta > 0.2N$.

The measures $p_{\rm sen}(i)$ and $p_{\rm spec}(i)$ give the accuracy of the method in extracting local connectivity information at each node. It would be interesting to study also the accuracy of the method in extracting the global features of a network. We

TABLE II. Dependence of $P_{\rm SEN}$ and $P_{\rm SPEC}$ on the parameters for the random network with consensus dynamics.

σ	g	$T_{\rm av}$	$P_{\rm SEN}$	$P_{\rm SPEC}$	Δ
0.01	0.1	1000	49.4	96.2	2.7
0.01	1	1000	87.7	98.0	7.1
0.01	10	1000	91.0	98.8	18.0
0.01	100	1000	97.7	99.3	30.1
0.1	0.1	1000	59.5	96.5	2.6
0.1	1	1000	99.6	99.7	17.1
0.1	10	1000	100.0	100.0	47.6
0.1	100	1000	100.0	100.0	72.6
1	0.1	1000	52.3	96.7	2.9
1	1	1000	99.8	99.95	22.2
1	10	1000	100.0	100.0	66.6
1	100	1000	100.0	100.0	80.4
1	0.1	10000	99.9	99.9	21.3
1	1	10000	100.0	100.0	67.1
10	0.1	1000	58.1	96.3	2.6
10	1	1000	99.7	99.9	22.1
10	10	1000	100.0	100.0	65.3
10	100	1000	100.0	100.0	80.4
100	0.1	1000	58.2	96.3	2.6
100	1	1000	99.7	99.9	22.1
100	10	1000	100.0	100.0	65.3
100	100	1000	100.0	100.0	80.4

concentrate on two global features: the degree distribution $P(k)$, which gives the fraction of nodes having degree k, and the eigenvalue spectrum, which gives the density of the eigenvalues of the adjacency matrix of the network. For scale-free networks, $P(k)$ has a power-law dependence on k: $P(k) \sim k^{-\alpha}$. Thus it is especially interesting to study how accurately the method can reproduce this power-law behavior of $P(k)$ for scale-free networks. The extracted degree of node i, denoted by $k_i^{(e)}$, is given by $\sum_j A_{ij}^{(e)}$. The fractional error of $k_i^{(e)}$ is related to $p_{\rm sen}(i)$ and $p_{\rm spec}(i)$ as follows:

$$\frac{k_i^{(e)}}{k_i} - 1 = \left(\frac{N-1}{k_i} - 1\right)\left[1 - \frac{p_{\rm spec}(i)}{100}\right] - \left[1 - \frac{p_{\rm sen}(i)}{100}\right]. \tag{24}$$

Therefore, with the same $p_{\rm sen}(i)$ and $p_{\rm spec}(i)$, the fractional error would be larger for nodes with smaller degree k_i. As a result, it is generally more difficult to extract accurately $P(k)$ in the small-k regime. We compare $P(k)$ using the extracted $k_i^{(e)}$ with the actual distribution using the actual k_i. As shown in Fig. 7, the extracted degree distribution resembles very well the actual degree distribution for all the three dynamics studied.

Next we study the accuracy of the method in obtaining the spectrum of eigenvalues of the adjacency matrix of a network. The eigenvalue spectrum gives important information about the topology of a network. The eigenvalues close to zero are shown to be related to weakly connected nodes, nodes that have a small degree [18]. On the other hand, the largest eigenvalue plays a significant role in determining whether an epidemic can spread on a network [19,20] and the value of the critical coupling for the onset of coherent behavior [21]. For the random network with $N \to \infty$, the density $\rho(\lambda)$ of the eigenvalues λ is given analytically by semicircle law [22]:

$$\rho(\lambda) = \begin{cases} \frac{\sqrt{4Np(1-p)-\lambda^2}}{2\pi Np(1-p)}, & |\lambda| < 2\sqrt{Np(1-p)}, \\ 0, & \text{otherwise}, \end{cases} \tag{25}$$

with the largest eigenvalue being pN. The eigenvalue spectrum of the BA scale-free network has been studied [23–25] numerically. The density of eigenvalues close to zero is found to be significantly larger than the semicircle law, and decays exponentially near the central peak and as a power law in the tail regions. The exponent of the power-law tail in the spectrum has been found [18] to be related to the power-law exponent α in the degree distribution $P(k)$. We check that the calculated actual eigenvalue spectrum for the random network and the BA scale-free network used in this work is in good agreement with the analytical semicircle law and the numerical spectrum obtained in Ref. [25], respectively. We calculate the extracted eigenvalue spectrum using $A_{ij}^{(e)}$, and compare it with the actual eigenvalue spectrum of $\hat{A}$. Results for the random network, the C. elegans network, and the BA scale-free network are shown in Figs. 8, 9, and 10, respectively. There is strikingly good agreement of the extracted eigenvalue spectrum with the actual one for all the cases shown in Table I. As a comparison, we show also the extracted eigenvalue spectrum from consensus dynamics in the small-g limit when the method does not give accurate results in Fig. 10. It can be seen that the density of small eigenvalues is underestimated while the density of intermediate eigenvalues is overestimated.

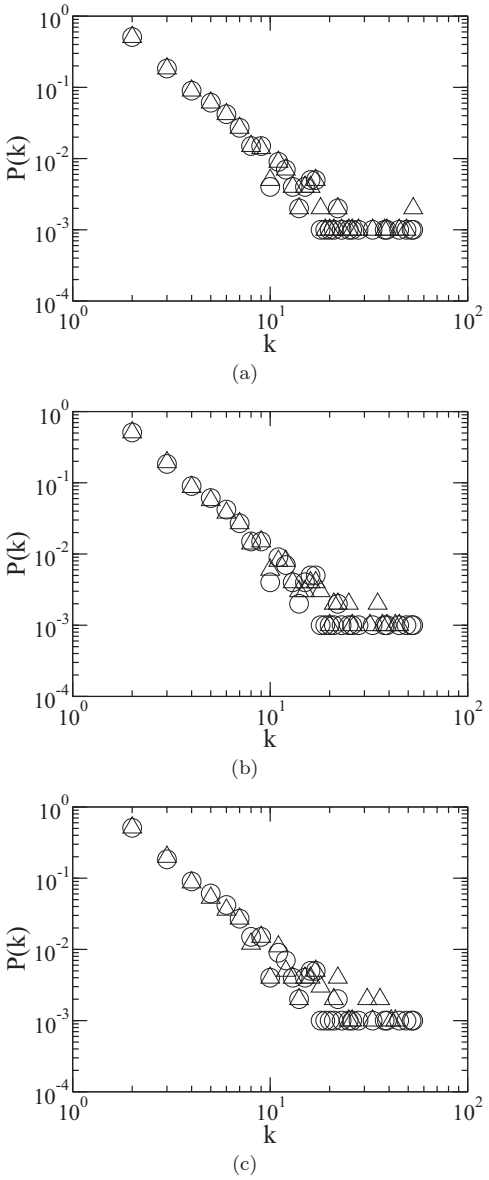

FIG. 7. Comparison of the degree distribution $P(k)$ calculated using $k_i^{(e)}$ (triangles) against the one calculated using the actual k_i (circles) for the BA scale-free network with (a) consensus dynamics with $g = \sigma = 1$, (b) FHN1 dynamics with $\sigma = 1$ and $g = 10$, and (c) FHN2 dynamics with $\sigma = 1$ and $g = 10$.

Finally, we explore the possibility to use the method to estimate the value of σ^2/g. If Eq. (10) holds, a straight line passing through the origin with a slope $\sigma^2/(2g)$ would be obtained when k_i is plotted against C_{ii}^+. The least-square-fit value of the slope is then given by $\sum_i^N k_i C_{ii}^+ / \sum_i^N (C_{ii}^+)^2$. Thus we can obtain an estimate of σ^2/g using this expression with k_i replaced by the extracted value $k_i^{(e)}$:

$$\left(\frac{\sigma^2}{g}\right)_{\rm est} = 2\frac{\sum_i^N k_i^{(e)} C_{ii}^+}{\sum_i^N (C_{ii}^+)^2}. \tag{26}$$

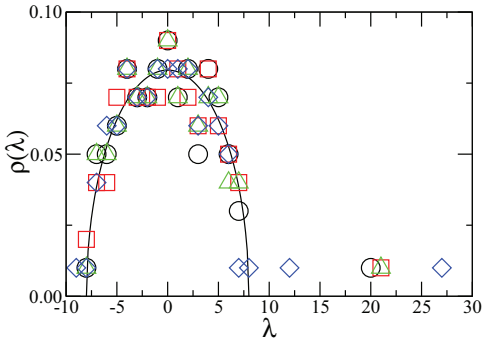

FIG. 8. (Color online) Comparison of the actual eigenvalue spectrum (circles) for the random network with $N = 100$ with the extracted eigenvalue spectrum for consensus dynamics with $g = \sigma = 1$ (squares), FHN1 dynamics with $\sigma = 1$ and $g = 10$ (triangles), and FHN2 dynamics with $\sigma = 1$ and $g = 10$ (diamonds), respectively. The analytical result for the actual spectrum for $N \to \infty$ is also shown as the solid line.

Such an estimate would be accurate if (i) Eq. (10) holds and (ii) the extracted values of $k_i^{(e)}$ are accurate. As discussed, the extracted values of $k_i^{(e)}$ are expected to be accurate when $\delta(i)$ are sufficiently large. Thus we measure how good condition (ii) holds using the value of Δ. It is clear that the validity of condition (i) cannot be checked as both k_i and σ^2/g are unknown in the first place. Thus we instead measure the goodness of fit of

$$k_i^{(e)} = \frac{1}{2}\left(\frac{\sigma^2}{g}\right)_{\text{est}} C_{ii}^{+} \tag{27}$$

using the coefficient of determination R^2, defined by

$$R^2 \equiv 1 - \frac{\sum_j \left[k_j^{(e)} - (1/2)(\sigma^2/g)_{\text{est}} C_{jj}^{+}\right]^2}{\sum_i \left[k_i^{(e)} - (1/N)\sum_j k_j^{(e)}\right]^2}. \tag{28}$$

The closer R^2 is to 1, the better is the fit of Eq. (27). Thus the necessary conditions for the estimate of σ^2/g to be accurate are Δ being large and R^2 close to 1. In Table III, we show the values of Δ and R^2 and the percentage error of the estimate $(\sigma^2/g)_{\text{est}}$. We see that, except for the three cases of scale-free networks studied, the estimate $(\sigma^2/g)_{\text{est}}$ is indeed accurate with a percentage error of less than 10% when both Δ is larger than 0.2 N and $R^2 > 0.9$. For the exceptional cases of the scale-free network, Eq. (27) is a good fit but the value of $(\sigma^2/g)_{\text{est}}$ deviates from the actual value of σ^2/g for more than 10%.

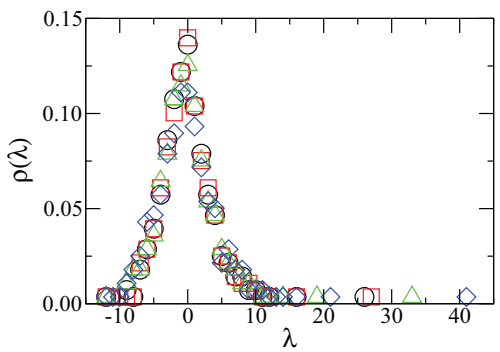

FIG. 9. (Color online) Same symbols as in Fig. 8 for the C. elegans network.

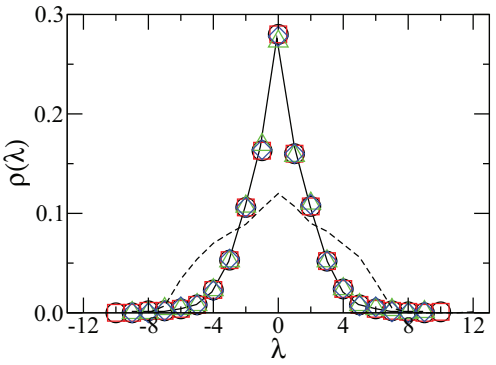

FIG. 10. (Color online) Same symbols as in Fig. 8 for the BA scale-free network. The solid line is the spectrum obtained numerically in Ref. [25]. As a comparison, we show also the extracted spectrum from consensus dynamics with a small $g = 0.1$ and the same $\sigma = 1$ (dashed line) for which our method does not give an accurate extraction.

V. CONCLUSION AND OUTLOOK

We have proposed an efficient method to extract the connectivity of networks in which the coupling is uniform and bidirectional using solely the dynamical time-series data of the nodes. Unlike earlier attempts, no additional input like the response dynamics to perturbations of the system [4] is needed. This appealing feature allows one to use the method in solving practical problems. Our method makes use of the separation of the ratio of the off-diagonal and diagonal terms of the pseudoinverse of the dynamic covariance matrix C_{ij}^{+} into two groups according to whether the nodes i and j are connected or not [Eq. (13)]. A noise-induced relation between the Laplacian matrix of the network and the dynamical covariance matrix of the nodes Eq. (8) provides the mathematical basis for such a separation. We have presented a direct derivation of Eq. (8) for networks with the consensus dynamics, that is, networks with nodes

TABLE III. Percentage error of the estimate $(\sigma^2/g)_{\text{est}}$.

Network	Dynamics	σ	g	Δ	R^2	Error (%)
Random	Consensus	1	10	66.6	0.996	5.8
Random	Consensus	1	1	22.2	0.994	0.2
Random	Consensus	1	0.1	2.9	0.140	38.2
Random	Consensus	0.01	1	7.1	0.530	3.1
Random	FHN1	1	10	48.5	0.989	1.4
Random	FHN1	1	1	2.4	0.698	52.2
Random	FHN1	0.1	10	9.0	0.708	9.4
Random	FHN2	1	10	30.7	0.790	27.8
C. elegans	Consensus	1	1	78.5	0.999	0.1
C. elegans	FHN1	1	10	72.1	0.960	0.3
C. elegans	FHN2	1	10	60.5	0.924	6.5
BA scale-free	Consensus	1	1	546.8	0.977	13.0
BA scale-free	FHN1	1	10	444.3	0.980	19.3
BA scale-free	FHN2	1	10	466.7	0.979	26.6

having no intrinsic dynamics and with linear diffusive coupling to one another. We have shown how the reference to the noise amplitude σ and coupling strength g in Eq. (8) can be eliminated to give Eq. (13), which forms the basis of our method.

We have demonstrated that our method can successfully extract both the local connectivity information of individual nodes as measured by the sensitivity and specificity, $p_{\rm sen}(i)$ and $p_{\rm spec}(i)$, and the global network properties of the degree distribution and eigenvalue spectrum of the adjacency matrix for a wide range of values of σ and g, when σ is larger than some threshold and when g is large. In the small-g regime, the accuracy of the method is only limited by the length of the time-series data. Although Eq. (8) has not been proved for systems with general dynamics, it has been found [8] that there is an approximate separation of the values of $\sigma^2/(2g)C^+_{ij}$ into two groups even for systems with chaotic Rössler dynamics [13]. [We have verified that our method works also for Rössler dynamics (results not shown).] This points to the general applicability of our method. Indeed, we have shown that our method works as well for networks with the nontrivial intrinsic FHN dynamics. Moreover, we can calculate the parameter Δ [or $\delta(i)$ for individual node i] using again only the input of time-series data, and assess the accuracy of the extracted information based on the value of Δ. Our results show that the method generally gives accurate results when $\Delta > 0.2N$. We have also explored the possibility of estimating σ^2/g by using Eq. (26). The estimate is generally accurate when both Δ is large ($\Delta > 0.2N$) and R^2 is close to 1 ($R^2 > 0.9$), but exceptions have been found for the BA scale-free network.

We anticipate that our method will be of value for application in realistic complex networked systems in which noise is inevitable practically. For example, in cultured cardiac cells or tissues, application of our extraction scheme to the time-series data on beating dynamics [26] or multielectrode array measurements can provide useful information on the structure and the noise-to-coupling ratio of the network. In the present work, we have considered networks with uniform, bidirectional linear-diffusive coupling. In realistic situations, coupling strength and/or noise amplitude can be different for different nodes and the coupling function can be nonlinear. Moreover, the connections can be directional as in networks of neurons. In addition, it is often impossible to collect data from all the nodes in the network. All these issues of heterogeneity of the network, directionality of coupling, and partial or missing information would make the extraction of networks in realistic problems more challenging. We are currently studying whether and how our method can be extended to tackle each of these complications. We have studied some simple forms of nonlinear coupling function such as $(x_j - x_i)^3$ and $\tanh[\alpha(x_j - x_i)]$, for some constant α, and found good results as well. We have found that it is possible to extend our method to networks with bidirectional coupling but with nonuniform coupling strength. Details of these results will be presented elsewhere.

ACKNOWLEDGMENTS

The work of P.-Y.L. has been supported by NSC of ROC under Grant No. NSC 101-2112-M-008-004-MY3, and NCTS of Taiwan.

APPENDIX: DERIVATION OF EQ. (8)

Equation (8) has been reported in [8] but, in the original derivation, $\hat{G}(t) = \exp(-g\hat{L}t)$ was mistakenly taken to be zero for $t \to \infty$, which leads to the erroneous result of $\hat{L}\hat{C} + \hat{C}\hat{L}^T = \sigma^2\hat{I}/g$, with the superscript T denoting the transpose of a matrix and $\hat{I}$ the identity matrix; then the solution of $\hat{L}\hat{C} + \hat{C}\hat{L}^T = \sigma^2\hat{I}/g$ was incorrectly taken to be Eq. (8). Here we present a direct derivation of Eq. (8). In vector form, Eq. (3) can be written as

$$\dot{\mathbf{x}} = -g\hat{L}\mathbf{x} + \eta. \tag{A1}$$

Since $\hat{L}$ is real and symmetric, it can be diagonalized by an orthogonal matrix $\hat{P}$:

$$\hat{P}^T\hat{L}\hat{P} = \hat{\Lambda}, \tag{A2}$$

where $\hat{\Lambda}$ is the diagonal matrix with $\Lambda_{ii} = \lambda_i$, and $0 = \lambda_1 < \lambda_2 \leqslant \cdots \leqslant \lambda_N$ are the eigenvalues of $\hat{L}$ in ascending order. As we consider networks whose graphs have only one connected component, $\hat{L}$ has only one null eigenvalue. Equation (A2) implies

$$\hat{L} = \hat{P}\hat{\Lambda}\hat{P}^T \Rightarrow \hat{L}^+ = \hat{P}\hat{D}\hat{P}^T, \tag{A3}$$

where $\hat{D}$ is the diagonal matrix with $D_{11} = 0$ and $D_{ii} = 1/\lambda_i$ for $i \neq 1$. Thus

$$L^+_{ij} = \sum_{k=2}^{N} \frac{P_{ik}P_{jk}}{\lambda_k}. \tag{A4}$$

Moreover, Eq. (6) implies

$$\begin{aligned} \Rightarrow 0 = \sum_{ij} L_{ij} &= \sum_i \sum_k P_{ik}\lambda_k \sum_j P_{jk} \\ &= \sum_k \lambda_k \left(\sum_j P_{jk}\right)^2 \Rightarrow \sum_j P_{jk} = 0, \quad \forall k \neq 1. \end{aligned} \tag{A5}$$

The solution of Eq. (A1) is given by

$$\begin{aligned} \mathbf{x}(t) &= e^{-gt\hat{L}}\mathbf{x}(0) + \int_0^t dt' e^{-g(t-t')\hat{L}}\eta(t') \\ &= \hat{P}\, e^{-gt\hat{\Lambda}}\, \hat{P}^T\mathbf{x}(0) + \int_0^t dt'\, \hat{P}\, e^{-g(t-t')\hat{\Lambda}}\, \hat{P}^T\eta(t') \end{aligned} \tag{A6}$$

or

$$\begin{aligned} x_i(t) = &\sum_{k,s} e^{-gt\lambda_k} P_{ik}P_{sk}x_s(0) \\ &+ \sum_{k,s} \int_0^t dt' \eta_s(t') e^{-g(t-t')\lambda_k} P_{ik}P_{sk}. \end{aligned} \tag{A7}$$

Using Eq. (A7), we get

$$\begin{aligned} \overline{X(t)^2} = &\frac{1}{N^2}\left[\sum_{l,k,s} e^{-gt\lambda_k} P_{lk}P_{sk}x_s(0)\right]^2 \\ &+ \frac{\sigma^2}{N^2}\sum_k I_k(t)\sum_l (P_{lk})^2, \end{aligned} \tag{A8}$$

$$\overline{x_i x_j} = \sum_{k,k',s,s'} e^{-gt(\lambda_k+\lambda_{k'})} P_{ik} P_{jk'} P_{sk} P_{s'k'} x_s(0) x_{s'}(0) + \sigma^2 \sum_k I_k(t) P_{ik} P_{jk}, \tag{A9}$$

$$\overline{x_i(t) X(t)} = \frac{1}{N} \sum_{l,k,k',s,s'} e^{-gt(\lambda_k+\lambda_{k'})} P_{ik} P_{lk'} P_{sk} P_{s'k'} x_s(0) x_{s'}(0) + \frac{\sigma^2}{N} \sum_k I_k(t) \sum_l P_{lk} P_{ik}, \tag{A10}$$

where

$$I_k(t) \equiv \int_0^t dt' e^{-2g\lambda_k(t-t')}. \tag{A11}$$

Here we have used Eq. (2) and the orthogonality of $\hat{P}$.

As a result, $\overline{[x_i(t) - X(t)][x_j(t) - X(t)]}$ can be written as the sum of two terms, $S_{ij}^{(1)}(t)$ and $S_{ij}^{(2)}(t)$. The latter contains all the terms proportional to σ^2 and the former contains the remaining terms. That is,

$$S_{ij}^{(1)}(t) = \sum_{k,k',s,s'} e^{-g(\lambda_k+\lambda_{k'})t} P_{sk} P_{s'k'} x_s(0) x_{s'}(0) \times \left(P_{ik} - \frac{1}{N}\sum_l P_{lk}\right)\left(P_{jk'} - \frac{1}{N}\sum_l P_{lk'}\right) \tag{A12}$$

and

$$S_{ij}^{(2)}(t) = \sigma^2 \sum_k I_k(t) \left\{ \frac{1}{N^2} \sum_l (P_{lk})^2 + P_{ik} P_{jk} - \frac{2}{N} \sum_l P_{lk}(P_{ik} + P_{jk}) \right\}$$

$$= \sigma^2 \sum_{k=1}^N I_k(t) \left(P_{ik} - \frac{1}{N}\sum_l P_{lk}\right) \times \left(P_{jk} - \frac{1}{N}\sum_l P_{lk}\right). \tag{A13}$$

Using Eq. (A5) and $P_{m1} = 1/\sqrt{N}$ for all m, we get

$$P_{ik} - \frac{1}{N}\sum_l P_{lk} = \begin{cases} 0, & k = 1, \\ P_{ik}, & k \neq 1. \end{cases} \tag{A14}$$

Therefore,

$$S_{ij}^{(1)}(t) = \sum_{k,k'=2} e^{-g(\lambda_k+\lambda_{k'})t} P_{ik} P_{jk'} \times \sum_{s,s'} P_{sk} P_{s'k'} x_s(0) x_{s'}(0), \tag{A15}$$

$$S_{ij}^{(2)}(t) = \frac{\sigma^2}{2g} \sum_{k=2}^N \frac{1 - e^{-2g\lambda_k t}}{\lambda_k} P_{ik} P_{jk}. \tag{A16}$$

In the limit $t \to \infty$,

$$S_{ij}^{(1)}(t) \to 0 \tag{A17}$$

and

$$S_{ij}^{(2)}(t) \to \frac{\sigma^2}{2g} \sum_{k=2}^N \frac{P_{ik} P_{jk}}{\lambda_k} = \frac{\sigma^2}{2g} L_{ij}^+ \tag{A18}$$

using Eq. (A4). Hence we finally get

$$C_{ij} = \langle \overline{[x_i(t) - X(t)][x_j(t) - X(t)]} \rangle = S_{ij}^{(1)}(t \to \infty) + S_{ij}^{(2)}(t \to \infty) = \frac{\sigma^2}{2g} L_{ij}^+, \tag{A19}$$

which is just Eq. (8). This result is exact in the limit of long-time averaging.

[1] S. H. Strogatz, Nature (London) **410**, 268 (2001).
[2] R. Albert and A.-L. Barabási, Rev. Mod. Phys. **74**, 48 (2002).
[3] M. E. J. Newman, SIAM Rev. **45**, 167 (2003).
[4] M. Timme, Phys. Rev. Lett. **98**, 224101 (2007).
[5] D. Yu, M. Righero, and L. Kocarev, Phys. Rev. Lett. **97**, 188701 (2006).
[6] S. G. Shandilya and M. Timme, New J. Phys. **13**, 013004 (2011).
[7] V. A. Makarov, F. Panetsos, and O. de Feo, J. Neurosci. Methods **144**, 265 (2005).
[8] J. Ren, W.-X. Wang, B. Li, and Y.-C. Lai, Phys. Rev. Lett. **104**, 058701 (2010).
[9] W. X. Wang, Q. Chen, L. Huang, Y. C. Lai, and Mary Ann F. Harrison, Phys. Rev. E **80**, 016116 (2009).
[10] R. Olfati-Saber, Proc. IEEE **95**, 215 (2007).
[11] The network of C. elegans neurons is obtained from the Wormatlas database (http://www.wormatlas.org/neuronalwiring.html). There are 279 neurons, and both chemical synapses and electric junctions are assumed to be bidirectional with the same coupling strength.
[12] A.-L. Barabási and R. Albert, Science **286**, 509 (1999).
[13] O. E. Rössler, Phys. Lett. A **57**, 397 (1976).
[14] R. FitzHugh, Biophys. J. **1**, 445 (1961).
[15] A. S. Pikovsky and J. Kürths, Phys. Rev. Lett. **78**, 775 (1997).
[16] C. Zhou, J. Kürths, and B. Hu, Phys. Rev. Lett. **87**, 098101 (2001).
[17] W. Y. Chiang, P. Y. Lai, and C. K. Chan, Phys. Rev. Lett. **106**, 254102 (2011).
[18] S. N. Dorogovtsev, A. V. Goltsev, J. F. F. Mendes, and A. N. Samukhin, Phys. Rev. E **68**, 046109 (2003).
[19] Y. Wang *et al.*, in *Proceedings of the 22nd International Symposium on Reliable Distributed Systems* (IEEE, Los Alamitos, CA, 2003), p. 25.
[20] M. Boguñá, R. Pastor-Satorras, and A. Vespignani, Phys. Rev. Lett. **90**, 028701 (2003).

[21] J. G. Restrepo *et al*., Chaos **16**, 015107 (2006).
[22] E. P. Wigner, Ann. Math. **62**, 548 (1955); **65**, 203 (1957); **67**, 325 (1958).
[23] R. Monasson, Eur. Phys. J. B **12**, 555 (1999).
[24] I. J. Farkas, I. Dereńyi, A.-L. Barabási, and T. Vicsek, Phys. Rev. E **64**, 026704 (2001); I. Farkas, I. Derenyi, H. Jeong, Z. Neda, Z. N. Oltvai, E. Ravasz, A. Schubert, A.-L. Barabási, and T. Vicsek, Physica A **314**, 25 (2002).
[25] K.-I. Goh, B. Kahng, and D. Kim, Phys. Rev. E **64**, 051903 (2001).
[26] W. Chen, S. C. Cheng, E. Avalos, O. Drugova, G. Osipov, P. Y. Lai, and C. K. Chan, Europhys. Lett. **86**, 18001 (2009).